Annual Review of Chaos Theory, Bifurcations and Dynamical Systems
Vol. 2, (2012) 32-54, www.arctbds.com.

Nonlinear Control and Chaotic Vibrations of Perturbed Trajectories of Manipulators

Przemyslaw Szumiński
Technical University of Lodz, Stefanowskiego 1/15, 90-924 Lodz, Poland
e-mail: Przemyslaw.Szuminski@lodz.pl.

Tomasz Kapitaniak
Technical University of Lodz, Stefanowskiego 1/15, 90-924 Lodz, Poland
e-mail: Tomasz.Kapitaniak@lodz.pl.

Abstract

We study different types of manipulators' attractors and propose a motion control method. In our analysis the manipulator's motion is perturbed and its stability investigated using the nonlinear equations of perturbations and linearized equations for practical control. In order to realize a practical control the common areas of stability for nonlinear and linear models are identified. The maps of stability calculated as functions of model parameters are proposed as a tool for motion control. The spectrum of Lyapunov exponents is introduced as a practical measure of motion quality. The procedure allows choosing a way of reaching system stability in order to avoid undesired attractors. Additionally, the possibility of the occurrence of strange chaotic attractors in manipulators, ways they appear, and codimension 2 bifurcations have been analyzed.

Keywords: Nonlinear vibrations, stability, Lyapunov exponents, manipulator.

Manuscript accepted June 20, 2012.

1 Introduction

The problems concerning mechanical vibrations of manipulators create an important issue in the manipulator design and its motion control. Numerous papers devoted to mechanical vibrations attempt answering the question, if and when vibrations of manipulator links occur during its motion [12-36]. These considered both, the theoretical and practical

aspects respectively, through investigations of single links, with a special emphasis on their flexibility for example [24-38]. Such methods have been usually based on classical equations of dynamics [20], most often in the form of equations of control [9-29-13].

The theory of nonlinear dynamics provides new possibilities of analysis of the dynamics and control of mechanical systems. The investigations that have been conducted allowing studies of new types of behavior in simple mechanical systems, such as vibrating oscillators by means of theory of bifurcations [16-43], spectrum of Lyapunov exponents, Poincaré maps [3-18]. In mechanical systems, chaos may lead to irregular operations and fatigue failure [8-25-31]. From this point of view the control of chaos is understood as a way to stabilize an unstable motion. Many papers show different ways of analysis of control in the case of nonlinear dynamics of manipulators. For example the papers by Caracciolo have proposed two control schemes that have been designed to achieve satisfactory performance in the position and vibration controlling of two closed-chain planar manipulators with flexible links. The control schemes have been designed, tuned and tested in simulation, where the dynamic behavior of the flexible manipulators have been reproduced through a fully coupled nonlinear model based on the finite element theory. The bifurcation control scheme may be implemented either with or without a feedback. In the latter case, we have the open-loop control. In static feedback control, the feedback is used to achieve desirable nonlinear dynamics when locations of equilibria are known [1-39]. When these locations are affected in the controlled system we can use dynamic feedback control [2-39]. In case of dynamic feedback control, it is possible to preserve the equilibrium positions in the controlled system.

In [4] the authors have examined open-loop control of chaotic dynamics of a nonlinear system by applying weakly periodic perturbations. One of the most popular approaches of chaos control is the method named Ott-Grebogi-Yorke (OGY) and proposed in [15-26]. In the OGY scheme, the control of chaos is understood as stabilization of unstable periodic orbits embedded in a chaotic attractor by application of appropriate small perturbations on a single system parameter. In order to achieve this task, the dynamics of the system is followed by analyze of the Poincaré map. The unstable point of periodic orbit on Poincaré map can be stabilized when the value of the modulus of the eigenvalues in the control matrix [26] is smaller than one. In the Pyragas method of chaos control [28], stabilizing of unstable periodic orbits has been applied by use of small time continuous control of a parameter of a system, while it evolves in continuously understood time. This method is known as delayed feedback control.

In [40] the authors have employed the time-delay feedback to anti-control of a permanent magnet DC (PMDC) motor system for vibratory compactors, and hence implement the new, electrically chaotic compactor. Firstly, the dynamic model of the anti-controlled PMDC motor system and the proposed electrically chaotic compactor have been formulated. Secondly, a nonlinear map have been derived in order to analyze the chaotic criterion of the anti-controlled PMDC motor system. Anti-control of chaos of single time scale brushless DC motor have been studied in [5]. Anti-control of chaos have been achieved by addition of an external nonlinear term. Then, by addition of some coupling terms, using the Lyapunov stability theorem and linearization of the error dynamics, the chaos synchronization between a third-order brushless DC motor and a second-order Duffing system have been presented. In the paper [23] a new technique of generating several independent

chaotic attractors by design a switching piecewise-constant controller in continuous-time systems has been shown. The controller can create chaos using an anti-control of chaos feedback. It has been shown that nonlinear continuous-time system can possess several attractors, depending on the initial conditions.

More detailed information about the stability analysis based on different assumptions can be found in [6-7-10-11-22-33-41].

The spectrum of Lyapunov exponents is a powerful tool of the analysis of the nonlinear system dynamics due to fact, its values easily illustrate exponential divergence or convergence of the trajectory on attractor [19]. The exponents describe logarithmic measure of the sensitivity of the dynamical system on arbitrary small changes in the initial conditions. Their computation is, however, time-consuming and generally complex for most of the nonlinear dynamical systems with more than one degree of freedom. Therefore, it is impossible directly employing this tool in the analysis of the motion. Some algorithms for calculation and mathematical description of Lyapunov exponents can be found in [17-18-19-25-42].

One of the reasons of limited use of nonlinear theories in technical applications is that, the numerical computations are often regarded as impractical. In the present paper, we suggest a method for the analysis of manipulator vibrations and nonlinear control based on the analysis of stability regions in the stability maps of the nonlinear and linearized system. The method allows controlling of the system in real time. Additionally, the presented method allows analyzing effects of changes of various parameters on the manipulator vibrations after a perturbation of its motion. We also propose a practical scheme of control, based on the so-called stability maps. The first step of the controlling method consists of the determination of critical values of manipulator's parameters for which a change in stability, i.e., a bifurcation, takes place. The idea of manipulator instability is understood as instability in the sense of Lyapunov [14-19]. Determining of the spectrum of Lyapunov exponents and the Poincaré maps have allowed successful investigation of asymptotic behaviour of the phase flow in the neighborhood of the trajectory after a perturbation. Then, nonlinear equations of the perturbations allow determination of the nonlinear regions of stability of the manipulator motion.

However, such a determination of requires exhaustive mathematical computations and cannot be used for control in practice. A linear stability of the manipulator is investigated by calculating, in real time, the eigenvalues of the Jacobian matrix in a close neighborhood of the perturbation point in the manipulator's nominal motion. As a result, the comparison of stability regions of the nonlinear and linearized systems allows determination of their common parts. For these subregions the ranges of system parameters corresponding to them are determined. The motion control is based on the selection of such control parameters for which the manipulator remains in the stability subregion. In practice, for the assumed ranges of perturbations, the stability subregions are stored in the control system memory in the form of a collection of maps. The actual measurements of perturbations allow for a practical selection of the control parameters from the collection (performed for assumed trajectory parameters). The determination of values of the parameters is ruled by a choice of the way the stability region is reached. It is connected with a specified bifurcation type, which takes place during the transition of the motion towards the stability region.

The advantage of the proposed method is a possibility of real-time motion control by analysis of nonlinear stability regions without any differentiation of the equations during the manipulator motion. Additionally, possibilities of occurrence of chaotic vibrations in the form of a strange chaotic attractor may be also investigated. The ways of a stability loss are investigated through the analysis of the bifurcation types [21-25-27-30-35-36-]. A theoretical analysis of nonlinear dynamics performed for the 7MAR manipulator is presented as an example.

2 Equations of perturbations, linear and nonlinear stability

The issue of stability of the motion becomes important when the gripping device motion becomes unstable for some parameters of the manipulator's model. Let us assume that the vector of the generalized coordinates of the links (the state vector) $\mathbf{q}(t,\varepsilon) = [q_{01}(t),\ldots,q_{0n}(t)]^T$, where n is a number of degrees of freedom of the links, is a solution to the autonomous equation of motion

$$\dot{\mathbf{q}} = \mathbf{F}(\mathbf{q},\varepsilon)\,, \tag{1}$$

where the state vector $\mathbf{q} \in R^{2n}$, the parameter vector $\varepsilon \in R^m$, Eq. (14), and the vector field $\mathbf{F}$ is defined for $R^{2n} \times R^m$. Let us perturb this solution. The vector of perturbation of the state vector has the form

$$\psi(t) = \mathbf{q}_p(t,\delta) - \mathbf{q}(t,\varepsilon)\,, \tag{2}$$

where $\varepsilon \in \delta$, δ is the vector of parameters of perturbation. A perturbation of motion of an arbitrary generalized coordinate can be described as

$$\psi_i(t) = q_{pi}(t,\delta) - q_{0i}(t,\varepsilon)\,, \tag{3}$$

where $\psi_i(t)$ describes a perturbation of the i-th generalized coordinate, $q_{pi}(t)$ is a perturbed motion of i-th generalized coordinate. The distance of the solution of the manipulator perturbed motion from the solution of the nominal motion is defined by $\mathbf{y}(t)$. Generally, the vector of perturbations which can appear during motion can be presented as

$$\mathbf{y} = \left[\psi_1, \dot{\psi}_1, \ldots, \psi_i, \dot{\psi}_i, \ldots, \psi_n, \dot{\psi}_n\right]^T . \tag{4}$$

Deflections of positions from the nominal motion and their time derivatives that appear in the mechanical system of the manipulator are compensated for by changes in values of the driving torques of the nominal motion. Let us write the vector of compensating driving quantities as

$$\boldsymbol{\Delta} = [\text{control system } 1,\ldots,\text{control system n}]^T . \tag{5}$$

The compensation vector $\boldsymbol{\Delta}$ is in practice a set of parameters of the control systems.

Substituting Eqs. (2) and (4), their derivatives and a vector of compensating quantities $\mathbf{\Delta}$ into the equations of motion, we obtain the dynamics equations of the perturbed motion

$$\dot{\mathbf{y}} = \mathbf{A}\mathbf{y} + \mathbf{B}\mathbf{\Delta} + \mathbf{N}\,, \tag{6}$$

where $\mathbf{y}$, $N \in R^{2n}$, $\mathbf{A}(\mathbf{q}, \dot{\mathbf{q}}, \ddot{\mathbf{q}}, \varepsilon) \in R^{2n\times 2n}$, $\mathbf{B}(\mathbf{q}) \in R^{2n\times n}$, $\mathbf{\Delta} \in R^n$. A Taylor series has been used to expand the trigonometric functions including components of the vector $\mathbf{y}$. A degree of nonlinearity of Eq. (6) depends on the form of the series expansion of the trigonometric functions. The matrix $\mathbf{N}(\mathbf{q}, \dot{\mathbf{q}}, \ddot{\mathbf{q}}, \mathbf{y})$ includes the nonlinear terms of the equations of motion (6). After the perturbation of the manipulator operation, its nominal motion has been eliminated from the perturbation equations due to the extraction of classical equations of dynamics of the nominal motion from them. Next, the equations of dynamics written for the nominal motion of the manipulator has been extracted from the perturbation equations, taking thus into consideration the manipulator's motion after perturbation. It is possible, due to the fact, the nominal motion is compensated for through the nominal driving torques of the drive systems. As a result Eq. (6) received the form

$$\dot{\mathbf{y}} = \mathbf{G}(\mathbf{y}, \mathbf{q}, \dot{\mathbf{q}}, \ddot{\mathbf{q}}, \varepsilon, \mathbf{\Delta})\,, \tag{7}$$

where $\mathbf{y} \in R^{2n}$, the parameter vector $\varepsilon \in R^m$, $\mathbf{\Delta} \in R^n$, the space function $\mathbf{G} \in R^{2n} \times R^n \times R^m$. One from the solutions of Eq. (6) has the form Eq. (8). This solution corresponds to the moment of motion perturbation.

2.1 Stability in the sense of Lyapunov

The problem of stability in the Lyapunov sense [18-30] of the gripping device motion is formulated as an analysis of stability of the equations of the perturbed motion, as a function of $\varepsilon, \mathbf{\Delta}$

$$\mathbf{y} = 0\,. \tag{8}$$

Lyapunov exponents associated with a trajectory are a measure of the average rates of expansion and contraction of the trajectories surrounding it. They are asymptotic quantities, defined locally in the state space, and describe the exponential rate, at which a perturbation to a trajectory of a system grows or decays with time at a certain location in the state space. The Lyapunov exponents calculated for the nonlinear system are described by [19-34]

$$\lambda_i = \lim_{t\to\infty} \frac{1}{t} \ln |m_i(t)|\,, \qquad i = 1, ..., 2n\,, \tag{9}$$

where all of the m_i are the eigenvalues of matrix of the fundamental solutions of linearized equation of perturbation. The procedure used to determine the Lyapunov exponents can be considered as a generalization of linear stability analysis. The Lyapunov exponents are global quantities associated with an attractor even though they are defined only locally in the state space. From this point of view the method of analysis of behaviour of the system will be called nonlinear.

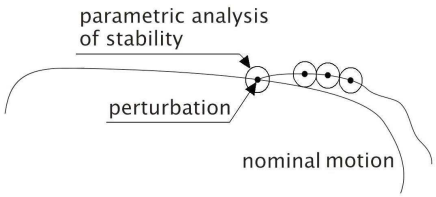

Figure 1: Discrete parametric analysis of the system behaviour in the close neighborhood of the perturbed motion.

2.2 Linear analysis of stability in close neighborhood of the moment of perturbation

In Fig. 1 an idea of the stability analysis in the neighborhood of the perturbed motion is presented.

It is possible to control the system by analysis of eigenvalues calculated in a close neighborhood of the trajectory. As a result of linearization of the Eq. (6) in the vicinity of the perturbation point $\mathbf{q}(t)$, the Eq. (7) has the form

$$\dot{\mathbf{y}} = \mathbf{A}^* \mathbf{y}\,, \tag{10}$$

where $\mathbf{A}^*(\mathbf{q}, \dot{\mathbf{q}}, \ddot{\mathbf{q}}, \varepsilon, \boldsymbol{\Delta})$ is the Jacobian matrix. As can be seen, the coordinates of the matrix $\mathbf{A}^*$ depend on the control system parameters, Eq. (5), on the manipulator's main parameters, Eq. (14), and on the generalized coordinates of the nominal motion of the manipulator's links.

Analysis of stability of the column matrix (8) is reduced then to the analysis of its eigenvalues. In order to perform this analysis, we have to generate the matrix $\mathbf{A}(t)$ composed of the derivatives of the equations of perturbed motion, Eq. (6), as a function of parameters of perturbations, Eq. (4), in the form

$$\mathbf{A}(t) = \frac{\partial f_i(\mathbf{y}_{i0})}{\partial \mathbf{y}_i} \tag{11}$$

for the set of conditions $\mathbf{y}_0$ for the given time instant and where Eq. (6) is $\dot{y} = f(y, t)$. The eigenvalues of the perturbation equations in the vicinity of the perturbation conditions can be determined from the determinant

$$\det[\mathbf{A}(t) - \boldsymbol{\Lambda}\mathbf{I}] = 0\,, \tag{12}$$

where $\mathbf{A}(t) \in R^{2n \times 2n}$ is the Jacobi matrix in the point $\mathbf{y}_0$, $\overline{\Lambda}$ – the vector of eigenvalues, and $\mathbf{I}$ – the unit matrix, $\mathbf{I} \in R^{2n \times 2n}$.

The roots of Eq. (12) determine regions of stability. The solution in the close neighborhood of the perturbation has tendency to be stable, if eigenvalues are negative or equal to zero. Analysis of the eigenvalues in the vicinity of perturbation point allows to determine the behaviour of the system in close neighborhood of perturbation. This behaviour shows tendency of the system to be / not to be stable. As a result we can determine parametric regions of stability. Analysis of the eigenvalues in vicinity of the perturbation point is linear analysis of stability.

2.3 Poincaré maps

Algorithms for the numerical continuation of the periodic solutions are quite sophisticated [2-22]. These algorithms have been extensively used for computing the forced response and limit cycles of the nonlinear dynamical systems.

The Poincaré maps in the paper were used as an additional tool for graphical presentation of stability areas of the nonlinear system. In the vicinity of the Eq. (8), the Poincaré map has been expressed as a set

$$\{[\psi_i(t), \dot{\psi}_i(t)]\,|_{t=t_0+k\cdot T}\,, i = 1, ..., n, k = 1, 2, ...\}\,, \tag{13}$$

where t_0 is the moment of the motion perturbation, T – the period of the gripping device motion along the trajectory of its motion.

As can be seen in Eq. (13), the procedure can not be used to control in the real-time motion.

2.4 Parametric analysis of stability

The stability analysis has been conducted in order to determine the stability regions. It has also consisted identification of influence of the manipulator's model parameters to a type of its behavior. These parameters can be divided into three groups. The first one concentrates on the kinematics of the gripping device, the second one is related to its motion trajectory, and the third one is discusses the stiffnesses and damping in the driving systems and rolling of the kinematics pairs. A set of the parameters that can to be investigated is

$$\varepsilon = \begin{bmatrix} \text{kinematics of gripping device} \\ \text{trajectory parameters} \\ \text{stiffness and damping} \end{bmatrix}, \tag{14}$$

where $\varepsilon \in R^m$. Some exemplary parameters of these groups have been presented in Sections 4.2 and 4.3. A selection of values of the set of parameters ε results in a defined type of the manipulator's behavior. Such a procedure allows finding a relationship between the set ε, defined by Eq. (14), and the type of manipulator's behavior, that is to say, the character of its oscillations.

3 Maps of stability subregions, stability control

Bifurcation maps of stability regions, performed on the basis of Eqs. (9),(13), are called maps of nonlinear stability of dynamical system. These maps have been made in function of a set of parameters of the Eq. (14). On the other hand, if we assume a close neighborhood of the matrix (8), then the linear analysis of stability in the vicinity of Eq. (8) using analysis of eigenvalues can be assumed as an approximation. This approximation affects manipulator's stability regions in an unknown way. Although the linearization helps determining whether a perturbation point is stable or not, it does not provide any information regarding the size of the domain around the perturbation point, where the conditions of stability holds. Therefore, in order to analyze the manipulator's stability

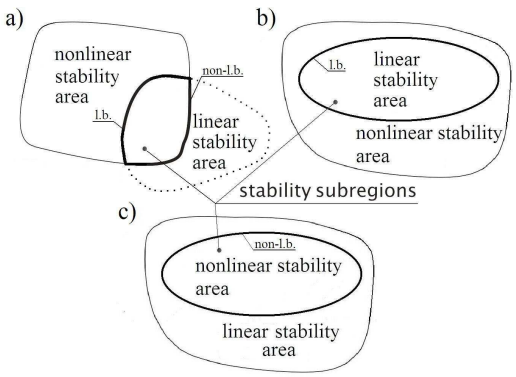

Figure 2: Ways of stability subregions analysis using map of the Lyapunov exponents for the assumed range of the motion perturbations. Description: (l.-b.) denotes the linear boundary of stability and (non-l.b.) the nonlinear one.

subregions, the analysis of stability regions for the nonlinear system using the linearized equations of perturbation has been suggested.

Generally, the ranges of parametric stability of the nonlinear and linear system do not correspond in the vicinity of the perturbation point. Therefore, it is proposed to separate the common parts of these regions (stability subregions). We can distinguish the following cases of the stability position of the nonlinear and linear system, (Fig. 2(a–c)):

(i) linear and nonlinear regions have a common part, Fig. 2a)

(ii) linear range inside the nonlinear range, Fig. 2b)

(iii) nonlinear range inside the linear range, Fig. 2c)

(iv) linear and nonlinear ranges without a common part: This situation is possible, if the correcting control signal appears in the control system in spite of absence of the motion perturbation, or, if the maps of the linear stability have been built for oversized ranges of the motion perturbations.

Maps of the linear stability have been constructed for certain ranges of the perturbations of the manipulator's state vector. Assumed ranges of the perturbations have decided about the size and position of the linear stability regions and about number of stability maps in the control system memory. As a result we have received the so-called stability subregions from the common part of the stability regions of the nonlinear system (by use of the Lyapunov exponents) and the linearized equations of perturbation in close neighborhood of the perturbation point (the vector of eigenvalues), Figs. 2(a–c).

Such a procedure allows avoiding of the effect of errors resulting from any simplification assumed in the mathematical model of the manipulator, and, first of all, for generation of the maps of the stability subregions as a function of ranges, in which the motion perturbations can occur. For a given map, the size of the stability subregions is related of course to the assumed perturbation ranges. In practice, in order to achieve the control of motion, it is easy to calculate the vector of eigenvalues and determine the values of the control parameters from the map of the stability subregions by simple measurement of the real perturbations. Of course, the set of such maps of the subregions stability should stay in the memory of the system control unit.

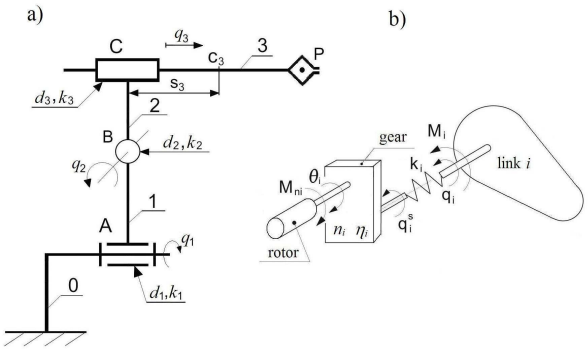

Figure 3: a) Kinematics scheme of the manipulator. b) Model of the driving systems, where n_i denotes the gear ratio, η_i the mechanical efficiency of the gear.

4 Model of the manipulator 7MAR

The 7MAR industrial manipulator, Fig. 3a, whose main data can be found in [36-], has been the subject to the numerical analysis. In order to determine the stability regions of the nonlinear and linearized systems, it is necessary to build the mathematical model of the manipulator and its drive systems. The model is important in the identification of nonlinear areas of the stability [19-36]. In the proposed method, the stability subregions that allow simplifications in the mathematical model have been separated from the common part of the stability regions of the nonlinear and the linearized systems. Generally speaking, the smaller the stability subregion in the stability zone, the more simplifications in the mathematical model, or, generation of a single map of stability regions for a higher range of motion perturbations are possible. The electric and mechanical model of the driving system of the manipulator covers the torsional flexibilities, viscous damping and resistance to friction in the driving systems. In Fig. 3b, the model of the driving systems is presented. It has been assumed that each link is driven by an independent driving system and consists of an electric motor, a mechanical gear and driving shafts. A stator of the driving motor of the i-th driving system is connected with the $(i-1)$-th link. Energy losses due to mechanical clearances in driving units and the gyroscopic effects between motors and manipulator links have been neglected.

The kinetic energy of the manipulator is defined by

$$E_k = \frac{1}{2}\left[\dot{\mathbf{q}}^T\mathbf{D}(\mathbf{q})\dot{\mathbf{q}} + (\dot{\mathbf{q}}^s)^T\mathbf{I}_{zr}\dot{\mathbf{q}}^s\right] , \tag{15}$$

where $\mathbf{D}(\mathbf{q})$ is matrix of inertia of the manipulator links, $\mathbf{I_{zr}}$ represents matrix of moments of inertia of rotors of the driving motors, power transfer shafts and rotating elements of the reductions gears reduced to the corresponding generalized coordinates of the links, $\mathbf{q}$ is vector of generalized coordinates of links, and, $\mathbf{q^s}$ is the vector of generalized coordinates of driving systems.

The potential energy of the manipulator has been expressed as a sum of the potential energy of links, an object being manipulated, elements of power transfer systems and flexibility in the driving systems. The potential energy of flexibility of driving systems is

described by a matrix of resultant torsional stiffnesses of the power transfer systems. The potential energy of the elements of the power transfer systems is equal to

$$E_p^d = \sum_{i=1}^{n}\sum_{j=1}^{l} E_{pij}^n = \sum_{i=1}^{n}\sum_{j=1}^{l_1} E_{pij}^n + \sum_{i=1}^{n}\sum_{j=l_1+l}^{l=l_1+l_2} E_{pij}^n \,, \tag{16}$$

where E_{pij}^n is the potential energy of the j-th element of the i-th manipulator driving system; l_1,l_2 are numbers of elements of the driving system of the link i assigned to the link $(i-1)$ and i, respectively.

The viscous friction in the driving system is a sum of the viscous friction in the driving motor and the viscous friction in the remaining part of the driving system reduced to the axis of the driving motor. Generally, for all the driving systems we have equations of motion in the form

$$\mathbf{I}_{zr}^* \ddot{\theta} + \mathbf{N}^{-1}\mathbf{K}(\mathbf{N}^{-1}\theta - \mathbf{q}) + \mathbf{B}\dot{\theta} = \mathbf{Q}_d \,, \tag{17}$$

where $\mathbf{N}$ is diagonal matrix of reduction gear ratios of driving systems; $I_{zr}^* = I_{zr}/N^2$ is the diagonal matrix of inertia of driving systems reduced to the corresponding axis of the driving motors; $\ddot{\theta}$ is vector of angular positions of rotors; $\mathbf{Q_d}$ describes the vector of the driving quantities of the links reduced to the axis of driving motors; $\mathbf{K}$ is the diagonal matrix of stiffnesses in the driving systems reduced to the corresponding generalized coordinates of the links; $\mathbf{B}$ represents diagonal matrix of viscous damping in the driving systems (notation d in Fig. 3) that has been expressed as follows

$$\mathbf{B} = \mathrm{diag}\left[f_{w1} + \sum_{l=1}^{w^1} f_{u1}^l,\ f_{wi} + \sum_{l=1}^{w^i}, f_{ui}^l, \ldots, f_{wn} + \sum_{l=1}^{w^n} f_{un}^l \right] , \tag{18}$$

where w^i states the number of elements of the i-th driving system that are considered in determination of viscous friction; f_{wi} is coefficient of viscous damping in the i-th driving motor; $\sum_{l=1}^{w^i} f_{w,un}^l$ represents sum of coefficients of viscous damping of individual elements of the power transfer system reduced to the axis of the i-th driving motor. Generally, the equations of motion of the manipulator assume the form

$$\mathbf{M}\ddot{\mathbf{q}}_m + \mathbf{C}(\mathbf{q}_m, \dot{\mathbf{q}}_m) + \mathbf{K}_g\mathbf{q}_m + \mathbf{G} = \mathbf{Q} \,, \tag{19}$$

where $\mathbf{M}$ is matrix of masses and inertia of the manipulator, $\mathbf{C}$ matrix of effects of gyroscopic forces, centrifugal forces and energy dissipation. $\mathbf{K}_g$ is matrix of the manipulator stiffnesses. The procedure of calculating the coefficients of stiffnesses can be found in [37]; $\mathbf{G}$ describes matrix of gravity forces; $\mathbf{Q}$ vector of the driving quantities; $\mathbf{q}_m = [\mathbf{q}, \theta]^T$ is the vector of generalized coordinates of the manipulator.

The manipulator performs its technological task in two steps. The first one means a motion in the first driving system and the second one a motion of the second and third degree of freedom, whereas the first degree is stationary. During the second step of motion, after introducing perturbations into second and third generalized coordinates Eq. (3) it has form

$$q_p = q_p + \psi_p \,, \quad \dot{q}_p = \dot{q}_p + \dot{\psi}_p \,, \tag{20}$$

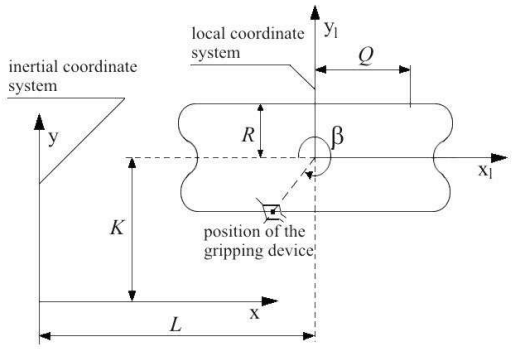

Figure 4: Parameters of the trajectory of the gripping device motion.

where $p = 1, 2$, we obtain nonlinear first order differential equations of the perturbations

$$\dot{\mathbf{y}} = a_{\mathbf{l}}\mathbf{y} + \mathbf{b_l}\boldsymbol{\Delta}_{\mathbf{n}} + \mathbf{c}^{\mathbf{2}}_{\mathbf{n}}(\mathbf{y}) + \mathbf{d}^{\mathbf{2}}_{\mathbf{n}}(\mathbf{y}, \dot{\mathbf{y}}) + \mathbf{c}^{\mathbf{3}}_{\mathbf{n}}(\mathbf{y}) + \mathbf{d}^{\mathbf{3}}_{\mathbf{n}}(\mathbf{y}, \dot{\mathbf{y}}) \tag{21}$$

where: $\mathbf{a}_l$, $\mathbf{b}_l$ are matrices of the linear parts of the equations of motion, $\mathbf{c}^2_n(\mathbf{y})$, $\mathbf{d}^2_n(\mathbf{y}, \dot{\mathbf{y}})$, $\mathbf{c}^3_n(\mathbf{y})$, $\mathbf{d}^3_n(\mathbf{y}, \dot{\mathbf{y}})$ are matrices of second and third order of the nonlinearity (depending on $\mathbf{y}$ and $\dot{\mathbf{y}}$), and, $\boldsymbol{\Delta}_n$ is the vector of compensating drive in the second and third driving system.

4.1 Trajectory and kinematics of the manipulator

The trajectory of the manipulator gripping device motion is presented in Fig. 4. We assumed periodic trajectory of motion as a typical trajectory of industrial machines. The position of the gripping device on its trajectory is described by an angle β in the local coordinate system $X_l Y_l 0_l$, see Fig. 4. It is possible to analyze the manipulator nominal motion as a function of an angle β.

4.2 Analysis of stability, bifurcations and strange chaotic attractors

The Lyapunov exponents are calculated for varying parameters of the velocity of the gripping device motion along the motion trajectory and for control parameters, Eq. (14). In the manipulator under consideration, the linear control has been applied. The model of the control system has the form

$$\Delta M_2 = aU_s\,, \quad \Delta M_3 = bU_s\,, \tag{22}$$

where ΔM_i, $i = 2, 3$ are the compensating driving quantities, U_s is the controlled variable (common for the second and third driving systems). The coefficient a is connected with the second drive system, whereas the coefficient b with the third drive system. The simplest algorithm of control allows showing, in an easy way, the spectrum of bifurcations which can be found also for more complex control systems [19]. The analysis has been

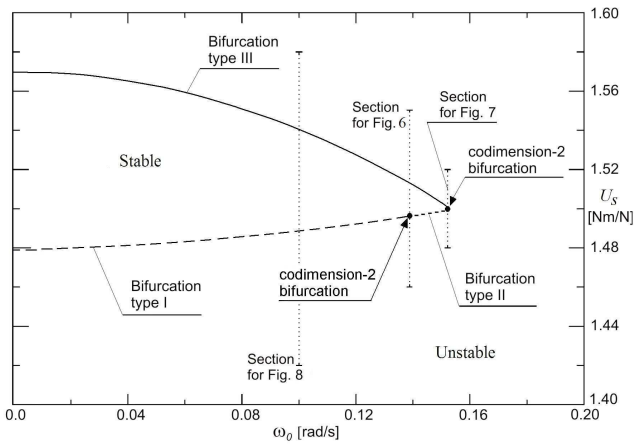

Figure 5: Stability as a function of control parameter U_s and the kinematics of the gripping device.

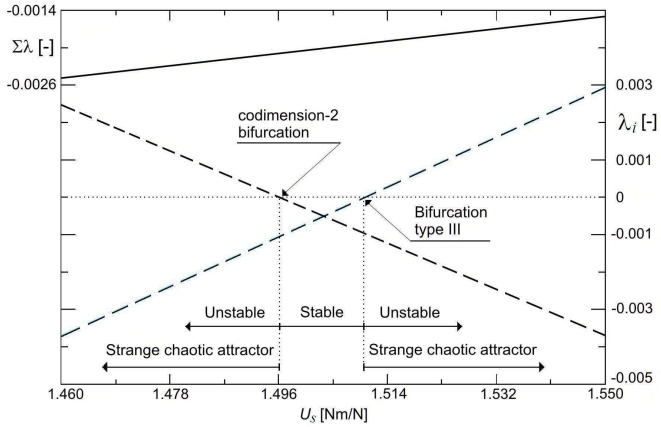

Figure 6: Spectrum of the Lyapunov exponents for the data presented in Figure 5 and $\omega = 0.1406$ rad/s.

conducted for the perturbations of positions and motion velocities of the second and third link. Below, a few sample diagrams of stability regions for the angle of the gripping device position $\beta = 5.5$ rad (perturbations occur at the instant when the gripping device is in this position, Fig. 4), are shown. The data concerning the motion trajectory of the gripping device are: $K = 0.5$ m, $L = 0.231$ m, $R = 0.05$ m, $Q = 0.05$ m. At the figures that show the spectra of the Lyapunov exponents, the broken lines represent two Lyapunov exponents.

In Fig. 5, a boundary of stability as a function of the control coefficient U_s and the angular velocity of the gripping device motion for the coefficients $a = -45.6$, $b = -0.003$ is depicted. The ranges of parameters for which the system is stable and the types of bifurcations which can occur during a loss of stability are seen. A selection of control parameters from the stability region allows for maintaining the motion stability in the Lyapunov sense. Each bifurcation allows one to identify vibrations that occur

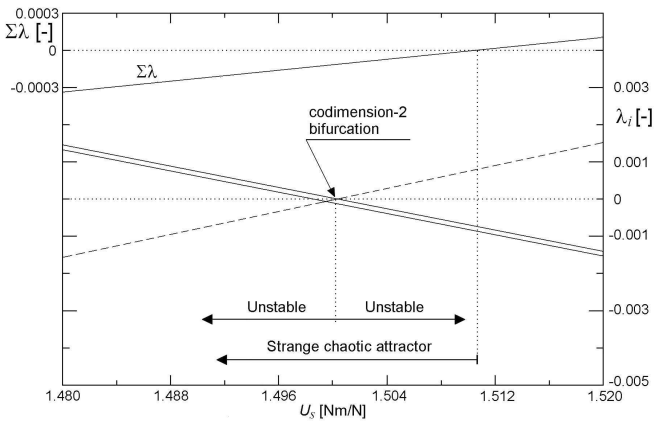

Figure 7: Spectrum of the Lyapunov exponents for the data presented in Figure 5 and $\omega = 0.1519$ rad/s.

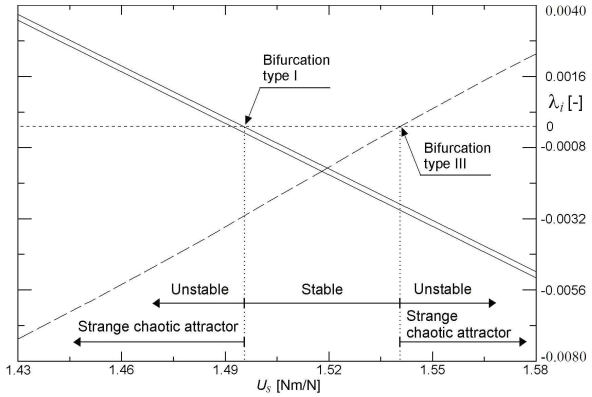

Figure 8: Spectrum of the Lyapunov exponents for the data presented in Figure 5 and $\omega_0 = 0.1$ rad/s.

after the stability loss of motion. Type I bifurcation is a saddle-node bifurcation. Type II bifurcation is a double-period bifurcation. In this case, the stable periodic trajectory with the period T is replaced by the trajectory with the period $2T$. Type III bifurcation is a secondary Hopf bifurcation [3-19-25]. In this case, the periodic solution transforms into a quasi-periodic one and, therefore, this type of bifurcation is the least disadvantageous from the point of view of the motion control.

Apart from this, it is seen in Fig. 5 that in the case of manipulators, bifurcations with codimension 2 can be found. In the first case of a codimension 2 bifurcation, the stability loss occurs due to the simultaneous occurrence of a saddle-node bifurcation and a double-period bifurcation. As can be seen in Fig. 6, in the bifurcation point, a decomposition of the 2-dimensional unstable torus that represents the quasi-periodic motion occurs. The torus decomposes and the motion along it is replaced by a motion on a strange chaotic attractor. In the second case, the stability loss is due to the simultaneous occurrence of a double-period bifurcation and a secondary Hopf bifurcation.

The stability loss takes place through a decomposition of the 3-dimensional unstable

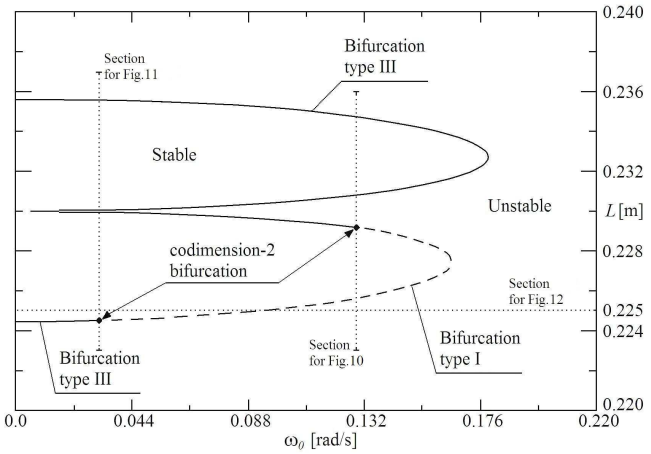

Figure 9: Stability loss as a function of the dimension L, Figure 4, and the kinematics of the gripping device motion.

torus, Fig. 7, that represents the quasi-periodic motion with three frequencies, between which there are no rational relationships. This mechanism leads to motions on strange chaotic attractors. As shown in Fig. 7, after the manipulator stability loss, a motion on the strange chaotic attractor occurs, but only for a certain variable of the driving system control. Above the value $U_s = 1.5108$ Nm/N, the system does not have an attractor, and the system shows a tendency towards the escape to infinity. An influence of the driving system control variable U_s on the stability and the character of motion after its stability loss is visible. In Fig. 8, a spectrum of Lyapunov exponents for the data from Fig. 5 and $\omega_0 = 0.1$ rad/s is presented.

The stability loss occurs through a saddle-node bifurcation and a secondary Hopf bifurcation. As a result of these bifurcations, unstable tori appear. As a result of their decompositions, the quasi-periodic motion is replaced by a motion on the strange chaotic attractor. This attractor is present in the whole unstable range of the system. In this case, the system has an attractor and because of this the loss of stability is not so disadvantageous. In Fig. 9, we can see a stability region and types of bifurcations as a function of the quantity L of the position of the motion trajectory, Fig. 4, and the velocity of motion of the gripping device along the trajectory of its motion. The following values of the control coefficients have been assumed: $U_s = 1.51$ Nm/N, $a = -45.6$, $b = -0.003$. An influence of the position of the trajectory of motion of the gripping device on the manipulator stability region and bifurcation type is visible. During the stability loss, it is possible that all three types of bifurcation with codimension 1 and a bifurcation with codimension 2 for $\omega_0 = 0.0316$ rad/s and 0.129 rad/s will occur. The bifurcation with codimension 2 is in this case a combination of a secondary Hopf bifurcation and a saddle-node bifurcation. The stability loss occurs through the occurrence and simultaneous decomposition of the unstable 3-dimensional torus. The spectrum of Lyapunov exponents for $\omega_0 = 0.129$ rad/s is shown in Fig. 10. As can be seen, such ranges are possible to occur when the system has a strange chaotic attractor, which however ceases quickly to exist. In practice, after the stability loss, the system does not have an attractor. A similar situation concerns

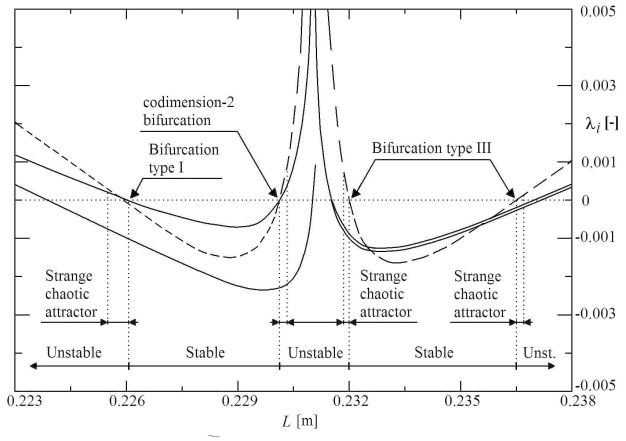

Figure 10: Spectrum of the Lyapunov exponents for the data presented in Figure 9 and $\omega_0 = 0.129$ rad/s.

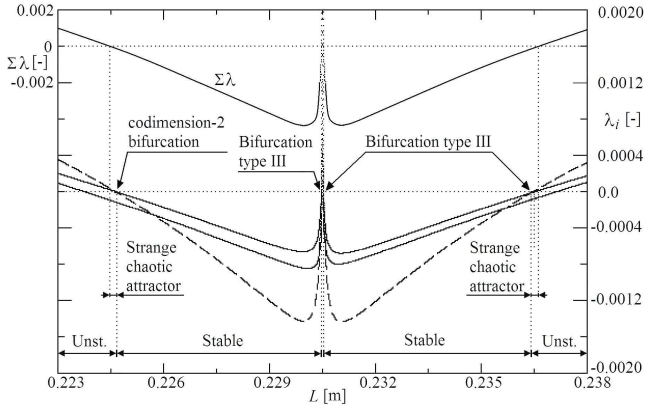

Figure 11: Spectrum of the Lyapunov exponents for the data presented in Figure 9 and $\omega_0 = 0.0316$ rad/s.

the second bifurcation point with codimension 2 ($\omega_0 = 0.0316$ rad/s), whose vicinity is shown in Fig. 11 in the form of the spectrum of Lyapunov exponents. The regions of stability and the ways of the stability loss are visible. Fig. 12, an influence of the angular velocity of the gripping device motion along the periodic trajectory on the stability regions and the ranges of occurrence of a strange chaotic attractor can be seen. Thus, both the control coefficients and the control variable, as well as the kinematics of the gripping device motion exert an influence on the way of the stability loss and the type of vibrations that occur after it. Vibrations that occur in the system accompany each kind of bifurcation. During the stability loss, a bifurcation with codimension 2 can occur. It is interesting to find this kind of bifurcation for such a system. For the defined sets of model parameters, two bifurcations occur at the same time. We tend to eliminate a possibility of such phenomena through maintaining the operation of driving systems within ranges of a stable motion.

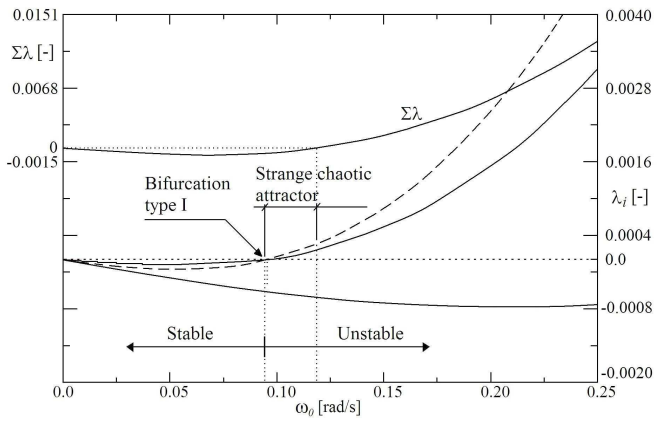

Figure 12: Spectrum of Lyapunov exponents for the data presented in Figure 9 and $L = 0.225$ m.

4.3 Maps of stability and control

In Fig. 13, a spectrum of the Lyapunov exponents as a map is proposed. This kind of map is introduced for choosing the values of control parameters for which the manipulator remains stable. The presented regions of stability are the resultant regions of stability obtained on the basis of the analysis of the nonlinear system (Poincaré maps, Eq. (13) and Lyapunov exponents Eq. (9)) and by means of the linearized equations of perturbation, Eq. (12). Besides, a way of transition from stability to a strange chaotic attractor as a function of the angular velocity of the gripping device motion and the control variable is presented. As can be seen, for a certain value of the angular velocity ω_0 that depends on the U_s, only a region without a manipulator attractor occurs. Below this velocity, a loss of stability leads to chaotic vibrations, regardless of the bifurcation type that causes this stability loss. Thus, there is a certain boundary value of the velocity ω_0 below which the system has an attractor and in which region of the control system should maintain the manipulator. A selection of values of the control parameters a, b from the range of a strange chaotic attractor gives rise to chaotic vibrations of the manipulator. As can be seen from the above-mentioned figures, the spectrum of Lyapunov exponents and the proposed maps of Lyapunov exponents are useful for control. Measures of perturbations which can occur during motion can be quickly presented in the form of the spectrum of their eigenvalues (the Lyapunov exponents). Next, from the maps of the stability subregions, it is easy to find for which values of control parameters the manipulator remains stable. On the other hand, Fig. 14 shows stability regions and types of induced vibrations as a function of the coefficients a and b for the control parameter $U_s = 1.51$ Nm/N and the angular velocity equal to 0.1 rad/s. In Fig. 14 two kinds of bifurcation with codimension 1 are possible: a saddle-node bifurcation and a secondary Hopf bifurcation. Apart from this, a bifurcation with codimension 2 is possible as well. Such a bifurcation with codimension 2 is composed of a secondary Hopf bifurcation and a saddle-node bifurcation.

The stability loss in the Lyapunov sense, resulting from the occurrence of this bifurcation, consists in the appearance and decomposition of a 3-dimensional torus. The quasi-periodic solution is unstable. Fig. 15 presents a map of Lyapunov exponents which

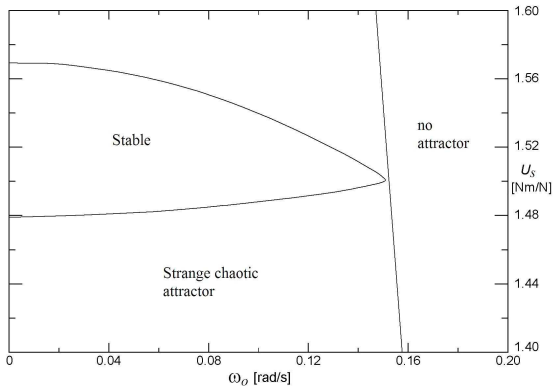

Figure 13: Map of stability and regions of strange chaotic attractors as a function of control parameter U_s and kinematics of gripping device.

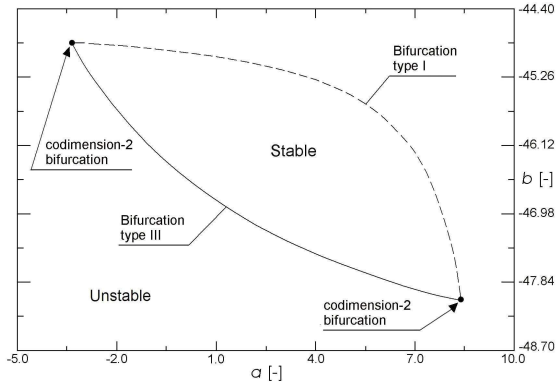

Figure 14: Stability losing as a function of control coefficients a and b.

shows a stable region and regions with a strange chaotic attractor or without it.

The ways of transition between the stable region and the remaining regions are interesting. A loss of stability by a bifurcation with codimension 2 is possible, Fig. 14, then vibrations occur on a strange chaotic attractor or the system escapes to infinity when the manipulator does not have an attractor. A loss of stability by a bifurcation with a codimension 1 leads to vibrations on a strange chaotic attractor.

In Fig. 16 a map which shows a way in which a stability loss leading to vibrations on a strange chaotic attractor occurs, regardless of the bifurcation co-dimension and its type, is shown. Narrow ranges of the values of control coefficients corresponding to the region of a strange chaotic attractor cause that the system escapes easily to the region where there is no attractor. In Fig. 17 a map of the regions of attractors for the gripping device position angle $\beta = 0.96$ rad is shown. In this case, we have only the regions with a strange chaotic attractor or the regions without an attractor. There is no stable region. A perturbation of the manipulator motion for the ranges of control coefficients shown leads to one of these regions and is particularly disadvantageous from the viewpoint of motion control.

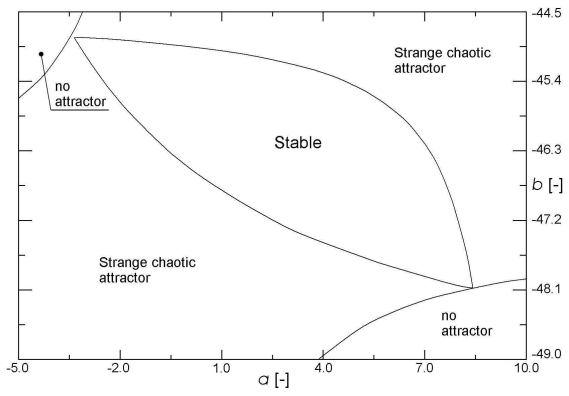

Figure 15: Map of stability and regions of strange chaotic attractors as a function of control coefficients a and b.

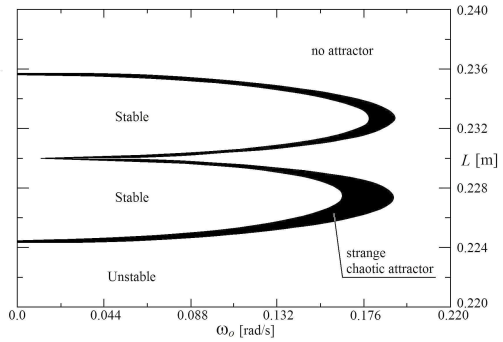

Figure 16: Map of stability and strange chaotic attractors regions as a function of the dimension L, Figure 4, and the kinematics of the gripping device.

Vibrations that occur in the system accompany each kind of bifurcation. During the stability loss of the model, a bifurcation with codimension 2 can occur. Finding this kind of bifurcation for such system is interesting. For the defined sets of model parameters, two bifurcations occur at the same time. The stability loss occurs through the decompositions of unstable, multidimensional tori that represent quasi-periodic vibrations. As a result, we obtain a strange chaotic attractor or a lack of the attractor, that is to say, a tendency of the system to the escape to infinity. We tend to eliminate a possibility of such phenomena occurrence through maintaining the operation of driving systems within ranges of a stable motion. A proper selection of values of control coefficients that depend on a perturbation allows for avoiding regions with a strange chaotic attractor or without it. In Fig. 18, an algorithm for the manipulator motion control has been proposed. This kind of control was qualified to nonlinear methods. The library in the control memory includes a set of stability maps drawn as a function of selected model parameters and as a function of perturbation ranges of individual degrees of freedom. The range of the coefficients a, b and the driving system control variable U_s and the positions of the trajectory, as well as the kinematics of the gripping device motion exert an influence not only on the motion stability but also on the character of motion after the stability loss. The stability loss of

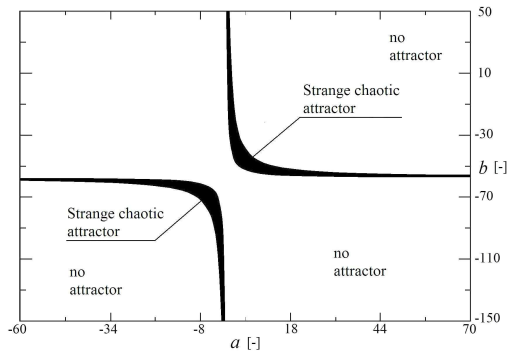

Figure 17: Regions of the strange chaotic attractors for the angle of the gripping device position $\beta = 0.96$ rad (Figure 4).

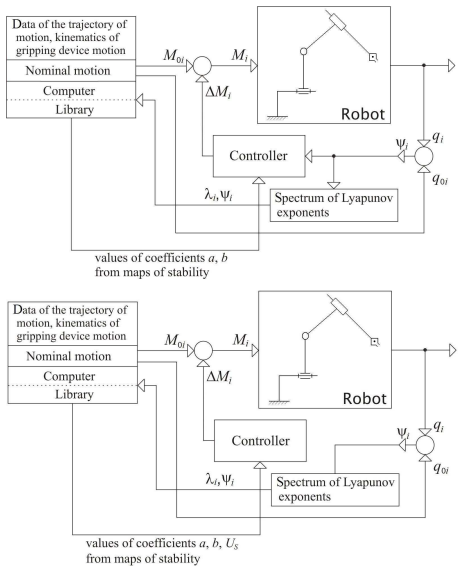

Figure 18: Schemes of the control systems.

the system should be avoided, however if it occurs, we should aim at the situation where the system has an attractor, even a chaotic one. It allows us to control the system during the stability loss. An idea of controllers used in the control systems is presented in Fig. 19. The controller defines a value of the moment ΔM, Eq. (22), on the basis of the coefficients a, b which are read from the correspond stability map. The control variable U_s is defined on the basis of measured perturbation ψ and some mathematical formula – Fig. 19a) or from map of stability which correspond to the value of perturbation – Fig. 19b).

As can be seen from the figures included in the paper, the analysis of the spectrum of Lyapunov exponents is a quick and simple method to parametric identify the stability regions in the Lyapunov sense, the threat of a loss of stability, the way the stability loss occurs and the kind of induced vibrations. From this point of view, it can be a valuable tool to control the motion. The proposed maps of Lyapunov exponents allow one to find

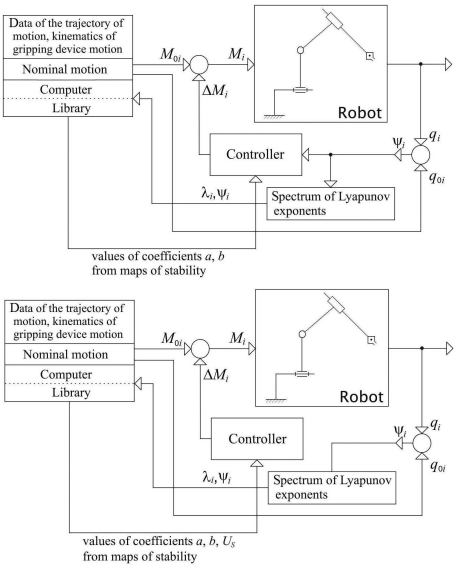

Figure 19: The controller loop with U_{si} linear depending on Ψ_i – a), and U_{si} taking from the map of stability - b).

values of control parameters for given motion perturbations. The main advantages of the proposed control rest on possibility of using this algorithm in real time despite of nonlinear analysis of the system.

5 Conclusions

In the paper a method of control of the manipulator motion from the nonlinear dynamics point of view is presented. The spectrum of Lyapunov exponents in the map form has been proposed as a tool to control motion. The control of motion is based on the analysis of stability regions of the nonlinear system and linearized equations of perturbation and on the generation of the so-called maps of stability. These maps are used in order to determine the values of control parameters, for which the manipulator remains stable after introducing perturbations to its motion. The method permits to control the nominal motion, to investigate the tendency towards a stability loss and to select a return way to the stability region by avoiding the chaotic vibration induction.

A method allows also for the parametric analysis of mode of vibrations. The algorithm allows for a theoretical analysis of an influence of manipulator model parameters on the ways the manipulator stability is lost and on the regions in which a strange chaotic attractor occurs or does not occur. A possibility of ways the strange chaotic attractor appear have been presented as well.

Acknowledgement

This paper is the last work of Dr. Przemyslaw Szumiński who died on 24 October 2011 at the age of 44.

References

[1] Abed, E.H. and Fu, H.-J., "Local feedback stabilization and bifurcation control. II. stationary bifurcation", *Systems Control Letters*, 8, 467-473, 1987.

[2] Abed, E.H., Wang, H.O., Chen, R.C., "Stabilization of period doubling bifurcations and implications for control of chaos", *Physica D*, 70, 154-164, 1994.

[3] Bishop, S.R. and Kapitaniak, T., The Illustrated Dictionary of Nonlinear Dynamics and Chaos, *J.Wiley & Sons*, London, 1999.

[4] Braiman, Y. and Goldhirsch, I., "Taming chaotic dynamics with weak periodic perturbations", *Physics Review Letters*, 66, 2545-2548, 1991.

[5] Caracciolo, R., Gasparetto, A., Giovagnoni, M., Trevisani, A., "On the control of flexible link manipulators: results of two numerical investigations", *Proceedings of the 12th International Workshop on Robotics in Alpe-Adria-Danube Region (RAAD'03)*, Cassino, Italy, 2003.

[6] Chen, S., Zhang, Q., Xie, J., Wang, C., "A stable-manifold-based method for chaos control and synchronization", *Chaos, Solitons and Fractals*, 20, 947-954, 2004.

[7] Ditto, W.L., Rauseo, S.N., Spano, M.L., "Experimental control of chaos", *Physics Review Letters*, 65, 3211-3214, 1990.

[8] Doedel, E.J., Keller, H.B., Kernevez, J.P., "Numerical analysis and control of bifurcation problems (I) Bifurcation in finite dimensions", *International Journal of Bifurcation and Chaos*, 1, 493-520, 1991.

[9] Dombre, E. and Khalil, W., Robot Manipulators. Modeling, Performance Analysis and Control, *Wiley–Blackwell*, 2007.

[10] Dressler, U. and Nitsche, G., "Controlling chaos using time delay coordinates", *Physics Review Letters*, 68, 1-4, 1992.

[11] Fuller, C.R., Elliott, S.J., Nelson, P.A., Active control of vibration, *Academic Press Limited*, London, 1996.

[12] Gawronski, W., Ih, C.H., Wang, S.J., "On dynamics and control of multi-link flexible manipulators", *Journal of dynamic Systems, Measurement, and Control*, 117, 134-142, 1995.

[13] Ge, Z.-M., Chang, C.-M., Chen, Y.-S., "Anti-control of chaos of single time scale brushless dc motors and chaos synchronization of different order systems", *Chaos, Solitons and Fractals*, 27, 1298-1315, 2006.

[14] Glendinning, P., Stability, Instability and Chaos, *Cambridge University Press*, 1995.

[15] Gonzalez-Miranda, J.M., Synchronization and control of chaos, *Imperial College Press*, London, 2004.

[16] Iooss, G. and Joseph, D.D., Elementary Stability and Bifurcation Theory, *Springer*, New York, 1981.

[17] Kapitaniak, T., Chaotic oscillations in mechanical systems, *World Science*, Manchester University Press, 1991.

[18] Kapitaniak, T., Controlling chaos, *Academic Press*, London, 1996.

[19] Kapitaniak, T., Chaos for engineers: theory, applications and control, *Springer-Verlag*, Heidelberg, 2000.

[20] Li, C. J. and Sankar, T. S., "Systematic methods for efficient modeling and dynamics computation of flexible robot manipulators", *IEEE Transactions of System Man and Cybernetics*, SMC-23(1), 77-94, 2006.

[21] Magnitskii, N. A. and Sidorov, S. V., "New methods for chaotic dynamics", *Scientific Series on Nonlinear Science A*, **58**, 2006.

[22] Manffra, E. F., Caldas, I. L., Viana, R.L., "Stabilizing periodic orbits in a chaotic semiconductor laser", *Chaos, Solitons and Fractals*, 15, 327-341, 2003.

[23] Morel, C., Bourcerie, M., Chapeau-Blondeau, F., "Generating independent chaotic attractors by chaos anticontrol in nonlinear circuits", *Chaos, Solitons and Fractals*, 26, 541-549, 2005.

[24] Nahvi, N. and Ahmadi, H., "Dynamic Simulation and Nonlinear Vibrations of Flexible Robot Arms", *Journal of Applied Sciences*, 3(7), 510-523, 2003.

[25] Nayfeh, A. H. and Balachandran, B., Applied nonlinear dynamics – Analytical, Computational, and Experimental Methods, *Wiley-VCH*, 2004.

[26] Ott, E., Grebogi, C., Yorke, J. A., "Controlling chaos", *Physics Letters Review*, 64, 1196-1199, 1990.

[27] Peeters, M., Viguie, R., Serandour, G., Kerschen, G. Golinval, J.-C., "Nonlinear normal modes, Part II:Toward a practical computation using numerical continuation techniques", *Mechanical Systems and Signal Processing*, 23, 195-216, 2009.

[28] Pyragas, K., "Continuous control of chaos by self-controlling feedback", *Physics Letters A*, 170, 421-428, 1992.

[29] Sciavicco, L., Modeling and control of robot manipulators, *Springer*, London, 2000.

[30] Seydel, R., Practical bifurcation and stability analysis, *Springer*, 2010.

[31] Shinbrot, T., "Chaos: Unpredictable yet controllable?", *Nonlinear Science Today*, 3, 1-8, 1993.

[32] Siciliano, B. and Sciavicco, L., Robotics: Modelling, Planning and Control, *Springer*, 2009.

[33] Sinha, S. C. and Joseph, P., "Control of general dynamic systems with periodically varying parameters via LyapunovFloquet transformation", *ASME Journal of Dynamcal Systems, Measurement, and Control*, 116, 650-658, 1994.

[34] Steeb, W. H., The nonlinear workbook, *Word Scientific*, 2008.

[35] Szumiński, P. and Kapitaniak, T. "Stability regions of periodic trajectories of the manipulator motion," *Chaos, Solitons and Fractals*, **17**: 67-78, 2003.

[36] Szumiński, P. and Kapitaniak, T., "Vibrations induced during a stability loss of periodic trajectories of the manipulator", *Machine Dynamics Problems*, 28(2), 65-85, 2004.

[37] Szumiński, P., "Determination of the stiffness of rolling kinematic pairs of manipulators", *Mechanisms and Machine Theory*, 42(9), 1082-1102, 2007.

[38] Tokhi, M.O and Azad, A.K.M., "Modelling of a single-link flexible manipulator system: theoretical and practical investigations", *Robotica*, 14, 91-102, 1996.

[39] Wang, H. O. and Abed, E. H., "Bifurcation control of a chaotic system", *Technical Report*, Institute of Systems Research, University of Maryland, Maryland, 1994.

[40] Wang, Z. and Chau, K. T. (2008). Anti-control of chaos of a permanent magnetic DC motor system for vibratory compactors. *Chaos, Solitons and Fractals*, **36**: 694-708.

[41] Wang, R. and Jing, Z., "Chaos control of chaotic pendulum system", *Chaos, Solitons and Fractals*, 21, 201-207, 2004.

[42] Wing-Kuen Ling, B., Ho-Ching Lu, H., Lam, H., "Control of chaos in nonlinear circuits and systems", *World Scientific Series on Nonlinear Science, Series A*, 64, 2009.

[43] Yu, P., "Closed-form conditions of bifurcation points for general differential equations", *International Journal of Bifurcation and Chaos*, 15, 1467-1483, 2005.